An Acad Bras Cienc (2022) 94(2): e20211071 DOI 10.1590/0001-3765202220211071
Anais da Academia Brasileira de Ciências | *Annals of the Brazilian Academy of Sciences*
Printed ISSN 0001-3765 I Online ISSN 1678-2690
www.scielo.br/aabc | www.fb.com/aabcjournal

MICROBIOLOGY

An experimental and *in silico* analysis of *Lacticaseibacillus paracasei* isolated from whey shows an association between lactate production and amino acid catabolism

CARLOS E. MEJÍA-GOMEZ, RIGOBERTO RIOS-ESTEPA, LUIS A. GONZALEZ-LOPEZ & NORMAN BALCAZAR-MORALES

Abstract: The production of lactic acid from agroindustry waste products, such as whey, heavily relies on microorganisms within the genus *Lactobacillus*. In this work, a genome-scale metabolic model was implemented from Vinay-Lara (*i*Lca334_548), improved adding some enzymatic reactions and used to analyse metabolic fluxes of *Lacticaseibacillus paracasei*, which is a *Lactobacillus* strain isolated from whey used in the large-scale production of lactic acid. Overall, the highest rate of lactic acid productivity was 2.9 g l^{-1} h^{-1}, which equates to a dilution rate of 0.125 h^{-1}, when continuous culture conditions were established. Restrictions on lactic acid production caused by exchange reactions, complex culture medium and intracellular metabolite concentrations were considered and included in the model. In total, the *i*Lca334_548 model consisted of 1046 reactions and 959 metabolites, and flow balance analysis better predicted lactate flux than biomass. The distribution of fluxes exhibited an increase in lactate formation as biomass decreased. This finding is supported by the reactions carried out by glyceraldehyde 3-phosphate dehydrogenase, pyruvate formate lyase and ribose-5-phosphate isomerase, corroborating the modelled phenotype with experimental data. In conclusion, there is potential for the improvement of lactate production in a complex media by amino acid catabolism, especially when lactate is derived from pyruvate.

Key words: flux balance analysis, genome-scale metabolic network model, lactate, lactic acid bacteria, whey.

INTRODUCTION

Lactic acid (LA) is an organic and massively consumed acid that is mostly in demand for the production of biodegradable polymers such as polylactic acid (PLA) (Castro-Aguirre et al. 2016, Research and Markets 2017). An alternative to satisfy this demand is transforming agro-industrial waste such as whey into LA, ethanol or probiotics (Alves et al. 2019, Ahmad et al. 2019).

The genus *Lactobacillus* is characterised as a group of bacteria with demanding nutritional requirements due to the environment from which they were isolated (Novák & Loubiere 2000, Wegkamp et al. 2010). In lactobacilli, after the entry of carbohydrate (e.g. lactose) into the microorganism, the metabolism is initiated, mainly via the phosphoenolpyruvate-sugar phosphotransferase system (PTS^{LAC}). This system involves the transport and phosphorylation of lactose at the expense of phosphoenol pyruvate (PEP) (Gänzle 2015) and determines carbon flow via the tagatose, glycolysis, pentose phosphate and pyruvate metabolic pathways. Pyruvate is the final product of glycolysis and depending on

the metabolic conditions of the cell, it may have different metabolic destinations. Thus, during anaerobic metabolism with limited substrate, the destination will be favoured by pyruvate formate-lyase (PFL) activity. In the presence of abundant substrate, lactate dehydrogenase (LDH) has the highest level of activity, resulting in high lactate production (Gänzle 2015, Ge et al. 2015). Additionally, the availability of oxygen in the medium can determine the orientation of pyruvate towards other compounds different from lactate, that determines the fermented product´s organoleptic properties (Zotta et al. 2017).

The complexity of cell metabolism demands a holistic approach for its study; mathematical modelling has greatly contributed to this aim (Panikov 2021). The development of a genome-scale metabolic network model (GEMs) (Feist et al. 2009, Machado 2018) for a specific organism allows the study of different metabolic scenarios resulting from a given environmental culture condition. By considering the stationarity nature of metabolic activity, it is possible to generate a system of algebraic equations whose solution represents the distribution of metabolic fluxes in the cellular system (Teusink et al. 2006, Durot et al. 2009, Feist et al. 2009, Vinay-Lara et al. 2014). In case of *Lactococcus lactis*, these GEMs revealed an interaction between branched-chain amino acids and the production of aromatics (Flahaut et al. 2013). Furthermore, for succinic acid production, the GEM predicted the phenotypic behaviour observed at an experimental scale and provided information on the use of economic carbon sources (Pereira et al. 2018).

Previous studies allowed the isolation, characterisation and establishment of optimal growth conditions for a *Lacticaseibacillus paracasei* (*L. paracasei*) strain present in whey (Mejia-Gomez & Balcazar 2020). These growth conditions are associated with the highly efficient production of LA. For *L. paracasei* in a medium with deproteinised whey, the main limitation was the poor use of amino acids present in the medium. In order to know the metabolic flows that require greater efficiency in lactate production, a flow balance analysis (FBA) was carried out based on the *i*Lca_334 model reported in the literature (Vinay-Lara et al. 2014), that was refined and used in the analysis of a *L. paracasei* strain associated with LA production from whey. The restrictions imposed by the nutrients present in the culture medium and the restrictions of the experimentally determined intracellular metabolites were included.

Flux balance analysis (FBA) contributes to the identification of enzymatic reactions susceptible to modification, which could lead to an increased LA production. Similarly, it contributes to the establishment of culture conditions that favour the direction of metabolic fluxes towards greater LA production using whey, which is a low cost and the same time, a highly polluting industrial waste of the dairy industry, as a base substrate.

MATERIALS AND METHODS

Microorganism growth and continuous culture

The strain (*L. Paracasei*) isolated from whey produced by a local dairy farm (Mejia-Gomez & Balcazar 2020) was grown in a modified DeMan-Rogosa-Sharpe medium (MRSM, lactose 20 g L^{-1}). By sequential transfers, the strain was moved to a deproteinised whey (DW) medium supplemented with 4 g L^{-1} of yeast extract (YE); this medium was called DW + 4. The continuous system was performed in a 3-litre reactor *Bioengineering Ralph*™ (Bioengineering AG, Switzerland) with a 2-litre working volume of DW + 4 medium at 37 °C, pH 6.0 and stirred at 100 rpm. The dilution rates evaluated were 0.05,

0.08, 0.125 and 0.20 h^{-1}. The experiments were done by triplicate.

Quantification of metabolites

LA and lactose were quantified using high-performance liquid chromatography (HPLC) in an Agilent® 1200 (Agilent Technologies, Santa Clara, CA, USA), using an HPX87H® Biorad (Bio-Rad Laboratories, Hercules, CA, USA) ion exchange column at 35 °C and a 5-mM mobile phase of H_2SO_4 at a flow rate of 0.6 mL min^{-1}. Lactose BioUltra® (Sigma-Aldrich, St. Louis, MO, USA), LA 88% (w/w) (Carlo Erba, Sabadell, Barcelona, España) and H_2SO_4 98% (w/w) (Mallinckrodt,St. Louis, MO, USA) were used for the standard curve.

Once the steady state was reached, 5-mL sample was added to 25 mL of methanol: water (60%) at -40 °C. The preparation was then mixed and centrifuged at 8.000 g for 5 min. The biomass collected was subjected to metabolite extraction with 500 µL of ethanol at 70 °C and incubated for 10 min at 90 °C with intermittent suspensions. It was finally centrifuged at 8.000 g for 3 min. The collected supernatant was stored at -80 °C until further testing (Gänzle et al. 2007, Pinu et al. 2017). The supernatant from 3 different experiments were pooled to intracellular metabolites determination.

Chromatographic separation of the compounds was conducted in a C-18 column Acclaim™ RSLC (Thermo Fisher Scientific, Waltham, MA, USA). Elution was performed using a gradient comprising (A) methanol and (B) 20 mM sodium formate, a flow of 0.15 mL/min and an injection volume of 10 µL. Intracellular metabolites were determined using an Impact II UHR–QqTOF mass spectrometer (Bruker, Billerica, MA, USA) at 40°C, with an orthogonal electrospray ionisation source. Nitrogen was used as a cone and desolvation gas, and the cone gas flow was 8 L min^{-1} (Luo et al. 2007). The metabolites quantified were: phosphoenol pyruvate (PEP); pyruvate (Pyr); erythrose 4 phosphate (e4p); glucose 1 phosphate (g1p); 6 phosphogluconate (6pgc); acetyl CoA (AcCoA); adenosine diphosphate (ADP); adenosine triphosphate (ATP) and nicotinamide adenine dinucleotide phosphate (NADPH).

Refinement of the GEM of *L. paracasei:* *i*Lca334_548 model

The bacterial strain used in the present work was identified as *Lacticaseibacillus paracasei* through analysis of the 16S rRNA gene. The development of the *i*Lca334_548 model used in this study, was based on the *i*Lca 334 model presented by Vinay-Lara for *L. casei* ATCC 334 (Vinay-Lara et al. 2014). The reversibility or irreversibility of the reactions was adjusted to the central carbon metabolism according to the KEEG (Kyoto Encyclopaedia of Genes and Genomes) pathway database resource (https://www.genome.jp/kegg/pathway.html). The carbohydrate source was lactose, and the nitrogen source was provided by the amino acids present in yeast extract and whey, according to the composition reported previously (Table SII). This model considered 548 genes, 1040 reactions and 958 metabolites. The model was refined and run using the Cobra toolbox; gaps were found thru the steady-state model and constraint consistency checker (MC3) (Yousofshahi et al. 2013). Additionally, the exchange reactions according to the dilution rates evaluated and irreversibility restrictions typical of the tagatose, glycolytic, pyruvate and pentose phosphate pathways were considered.

The restrictions imposed by the DW + 4 culture medium were added, that contained approximately 50 g L^{-1} of lactose and an amino acid composition relative to the concentration of 4 g L^{-1} YE. The upper and lower limits of the exchange reactions for other carbohydrates

were set at 0. The reactions involved restrictions due to intracellular concentration metabolite are listed in Supplementary Appendix S2 (Biomass equation (bio06001)). The *i*Lca334_548 model was converted to SBML format, which is compatible with the Cobra Toolbox software from Matlab™ (Navid 2021, Schellenberger et al. 2011).

Objective function selection

For the selection of the objective function, the maximisation of biomass formation flux, lactate flux and the combination of biomass and lactate flux were considered (Supplementary Appendix S1 - Objective function selection) (Schellenberger et al. 2011)

Model validation and Robustness analysis of iLca334_548 model in DW + 4 medium

The *i*Lca334_548 model was validated against experimental data for continuous cultures taken from literature and batch cultures under similar conditions for some lactobacilli (Table SIV). The model was tested for robustness (Edwards & Palsson 2000, Edwards et al. 2001) to assess the response in growth rate to changes in C:N ratio and different oxygen flows. For details see (Supplementary Material - Figure S1).

In-silico amino acids assimilation using iLca334_548 model

The percentage of assimilation of each amino acid, obtained from the equation: amino acid flux in vector solution over amino acid flux defined in lower bound (flux aa.x/flux aa.lb*100) was calculated in two different scenarios (with and without restrictions due to metabolite intracellular concentration) at different dilution rates.

Constrains-based Flux balance analysis with the *i*Lca334_548 model

The *i*Lca334_548 model was run under Matlab environment using the Cobra Toolbox, using the Gurobi 7.0 solver. Biomass synthesis was used as objective function (Supplementary Appendix S1 - Objective function selection). The flux distribution map in the central metabolism was presented together with the percentage of each flow regarding the lactose flow introduced, according to the equation, flux % = (reaction flux i/lactose flux) × 100. The first metabolic map that was generated considered only restrictions caused by exchange reactions, whereas the second, in addition to these reactions, considered the restrictions of the reactions that involved the intracellular metabolite concentrations, determined experimentally, that provided a feasible solution.

RESULTS

Microorganism growth and continuous culture

Samples were taken during the steady state of the continuous culture to determine the concentration of extracellular metabolites at different dilution rates. A maximum productivity of 2.87 g $(L\ h)^{-1}$ was acquired at a dilution rate of 0.125 h^{-1} (Table I). There was homolactic metabolism at different dilution rates ($Y_{P/S}$ 1 g g^{-1}) except at the 0.2 h^{-1} dilution rate, where a $Y_{P/S}$ of 1.76 was achieved ($Y_{P/S}$: gram of LA produced per gram of substrate consumed), the LA produced at this dilution rate was only 8.64 g L^{-1}, suggesting that the reactor was at the wash out rate conditions. The low substrate conversion (11%) and the fall in biomass formation were due to a decrease in residence time. Growth was limited by lactose depletion ($Y_{X/S}$ » 0.1 g g^{-1}) at the 0.05 and 0.08 h^{-1} dilution rates. The best substrate yield in biomass ($Y_{X/S}$ = 0.35 g g^{-1}) was

Table I. Kinetics of *Lacticaseibacillus paracasei* continuous culture.

D (h^{-1})	S_0 (lactose) g l^{-1}	S (lactose) g l^{-1}	Conv. (lactose) %	X (biomass) g l^{-1}	$Y_{X/S}$ g g^{-1}	P (Lactic A.) g l^{-1}	$Y_{P/S}$ g g^{-1}	Productivity g (l h)$^{-1}$	Specific Productivity g (l h)$^{-1}$ g^{-1}
0,05	50,99 ± 0,20	13,44 ± 0,23	74	2,60 ± 0,33	0,07	41,73 ± 0,15	1,11	2,09	0,80
0,08	48,40 ± 0,20	20,96 ± 0,04	57	3,84 (ND)	0,14	32,12 ± 0,32	1,17	2,57	0,70
0,125	49,81 ± 0,11	30,26 ± 1,45	39	7,07 ± 0,93	0,36	18,99 ± 1,60	0,97	2,37	0,34
0,20	45,27 ± 0,75	40,35 ± 0,19	11	0,92 (ND)	0,19	8,64 ± 0,46	1,76	1,73	1,88

D: dilution rate; S_0 (g l-1) substrate, at the beginning of fermentation (t = 0); S (g l^{-1}), X (g l^{-1}) and P (g l^{-1}) substrate, biomass and product respectively, at the end of fermentation. $Y_{X/S}$: substrate yield in biomass; $Y_{P/S}$: substrate yield in product. The values (S_0, S, X and P) represent the mean ± SE, n=3. ND: Non-determined.

achieved at the dilution rate of 0.125 h^{-1}, which matches the point of highest productivity.

Quantification of intracellular metabolites

The intracellular metabolite concentration is shown in Table II. At a dilution rate of 0.2 h^{-1}, the concentration of most intracellular metabolites decreased because of the high feed flow (F, L h^{-1}), indicating that the reactor reached the washing zone of the process. The intracellular metabolite concentrations were used to define the metabolic fluxes that established new restrictions in the *i*Lca334_548 model.

Characteristics of the GEM of *L. paracasei:* *i*Lca334_548 model

After the refinement process, the *i*Lca334_548 model contained 1046 reactions, 959 metabolites and other model check parameters as specified in Table SIII. Six reactions were added as follows: two reactions of the pentose phosphate pathway, one ATP hydrolysis reaction, one pyruvate (malate dehydrogenase) metabolism reaction and two-ethanol transport reactions. The biomass equation, used in this study, was the one defined by Vinay-Lara reaction bio06001 (Supplementary Appendix S2 - Biomass equation (bio06001)).

Objective function selection

Figure 1a and Table SI shows that when the objective functions biomass, biomass-lactate and lactate flux maximised, SGRs of 0.1, 0.04 and 0.02 h^{-1} were obtained, respectively. The objective biomass function was close to the SGR of 0.19 h^{-1} obtained experimentally (Mejia-Gomez & Balcazar 2020). When comparing the lactose flux with the SGR of the model, using the objective biomass function a hyperbolic and asymptotic behaviour was observed that is typical of the physiology of the growth of microorganisms versus the availability of carbon source (Fig. 1b). When the target lactate function was used, no significant change in SGR was observed in the initial lactose flux, but a rapid increase was observed for fluxes >2 mmol g^{-1} h^{-1} that did not resemble hyperbolic behaviour (Fig. 1b). When lactate fluxes were used as a response variable to lactose flux, no differences were observed between the objective biomass and lactate flux functions (Fig. 1c). Thus, biomass synthesis was selected as the objective function.

Both experimental and simulated lactate flux percentages, which were calculated based on the lactose fed, were close to the stoichiometrically equivalent flux (400%), see

Table II. Intracellular metabolite concentration for *Lacticaseibacillus paracasei* at different dilution rates.

	Dilution rate (h^{-1})			
	0,05	**0,08**	**0,125**	**0,2**
Pyruvate (pyr)	9,11	17,73	9,81	8,28
Phosphoenolpyruvate (PEP)	1,62	1,19	0,65	1,29
Eritrose-4-phosphate (e4p)	0,17	0,18	0,05	0,086
Glucose 1 phosphate (g1p)	0,87	0,54	2,9	0,03
6 Phosphogluconate (6pgc)	2,55	0,06	0,76	0,37
Acetyl CoA (AcCoA)	0,41	0,15	0,24	0,11
ADP	3,33	1,86	0,13	0,33
ATP	1.89	2,92	0,93	0,79
NADPH	2,07	2,27	1,37	1,47

The concentration of metabolites is given in uM and were determinate from pools of three independent experiments.

Table III. The experimental flux was above stoichiometric flux at dilution rates of 0.05 and 0.08 h^{-1}, possibly due to the assimilation of some amino acids for pyruvate formation and then lactate formation. The increase in lactate levels may also be caused by endogenous metabolism, determined by high retention times (20 and 12.5 hours, respectively).

At the dilution rate of 0.2 h^{-1}, the experimental data showed an inconsistency in the lactate flux percentage, which unreasonably exceeded the stoichiometric limits defined by lactose flux. The latter was found in only 4.92 g L^{-1} of the lactose consumed (Table I), indicating that it is in the wash zone because of such low lactose consumption.

In-silico determination of amino acids assimilation using the iLca334_548 model

The amino acids serine, arginine, aspartate, alanine and glycine showed an assimilation rate greater than 80% (Fig. 2a) when we did not account for the experimentally-determined intracellular concentration of metabolites as constraints. Similarly, these amino acids showed a greater rate of assimilation when the total concentration of intracellular metabolites was considered (Fig. 2b). However, in this case, the assimilation rate ranged from 20 to 50%.

When amino acid assimilation levels were compared at different dilution rates and the intracellular metabolism was not considered, we observed a generalised decrease in the assimilation of all amino acids at a dilution rate of 0.08 h^{-1}, except for aspartate. At this same dilution rate, higher assimilation rates are observed compared to those identified at the other dilution rates when intracellular metabolism is considered. From another perspective, similar amino acid assimilation rates were observed in the two simulations when the dilution rate was 0.08 h^{-1} (Fig. 2a-b).

Constrains-based Flux balance analysis using the *i*Lca334_548 model

At dilution rates of 0.05, 0.08 and 0.125 h^{-1}, there was a similar flux of carbon to lactate (»390, percentage of molar flux with respect to the lactose entered). A different flux was found at the dilution rate of 0.2 h^{-1}; this might be because, at this dilution rate, the culture is in the reactor wash zone and gives rise to different results as opposed to that at the other rates (Fig. 3b). For example, a 32% flux of biomass was reached

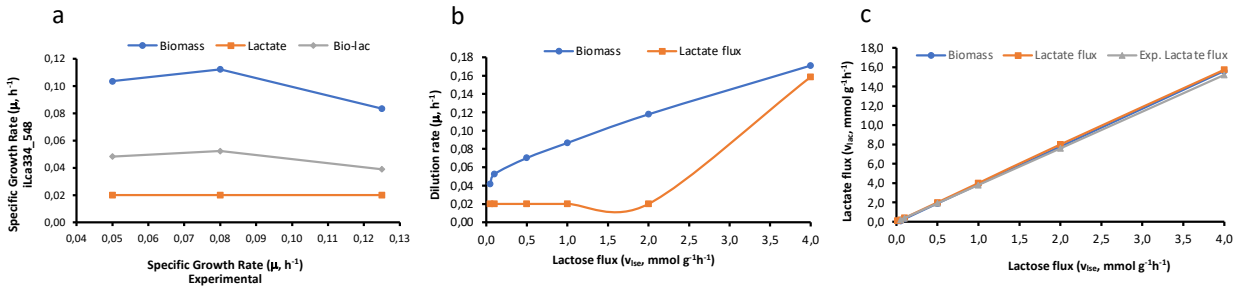

Figure 1. Selection of the objective function. a) Modelled specific growth rate (SGR) on the *i*Lca334 model against experimental SGR of *Lacticaseibacillus paracasei* at different dilution rates and evaluation of different objective functions. b) The effect of lactose fluxes on biomass and lactate flux on the *i*Lca334_548 model. c) The effect of change in lactose flux on the objective functions evaluated. C: N ratio of 5: 1 and dilution rates: 0.05, 0.08, 0.125 and 0.20 h^{-1}. Bio-lac: Biomass and lactate flux. Exp.: Experimental.

for this rate, while it did not exceed 8% for the other rates; the latter item is more acceptable in experimental terms for the genus *Lactobacillus*. In addition, a decrease in lactate flux at the 0.2 h^{-1} dilution rate compared to the other rates was evidenced (323 against » 390). This may be due to the deviation of flux through the PFL pathway that reached a flux of 35% for the rate of 0.2 h^{-1}. Furthermore, the flux through ribulose 5 phosphate isomerase (R5PI), an intermediate during biomass production, supports the explanation why such a high flux occurs in the synthesis of biomass in the model at 0.2 h^{-1} dilution rate (Fig. 3e).

The simulation results for the strain *L. paracasei* showed a similar trend to that of the experimental data (Table III), where the model tended to yield results below the stoichiometric maximum (400%) for percent lactate flux. The trend for the experimental data, mainly for lactate formation, was above the maximum, which might be caused by the formation of pyruvate from a substrate that is different from the one used in the glycolytic pathway. The reaction of serine to pyruvate is present in the model (rxn00165) and it is functional because a specific part of the pyruvate flux comes from that reaction (Teusink et al. 2006).

In general, the flux distributions obtained with the restrictions imposed by the concentration of intracellular metabolites at each dilution rate are similar (Fig. 4), with the exception of the 0.2 h^{-1} dilution rate, where a correlation between high biomass formation and high flux direction through R5PI was determined (Fig. 4e). In addition, it showed a lactate flux rate of approximately 400%, but a significant drop in the flux of biomass formation that reached 3% (Fig. 4a). The model shows correlation between high lactate production and low biomass production, responding to the logic of the nodal point of PFL, where no other organic acids appear (Fig. 4d).

Thus, the *i*lca34_548 model responded to the target biomass formation function, where the amino acids provided by the YE at the defined concentration, played an important role in maintaining the carbon:nitrogen ratio (5:1). Central carbon metabolism of *L. paracasei* showed a complete conversion of lactose into lactate, under the growth conditions studied in the continuous system.

Table III. Comparison of lactate flux and biomass synthesis for *Lacticaseibacillus paracasei* and *i*Lca334_548 model.

D (h^{-1})	Lactose flux[a]	Exp.[b] Lactate flux.	Simulated Lactate flux.	μ Simulated. (h^{-1})	Simulated Lactate flux (%).	Exp.[b] Lactate flux (%).	Simulated biomass (%)	Exp.[b] biomass (%).
0,05	2,1096	8,8959	8,3347	0,0507	395	422	2,4	2,4
0,08	1,6700	7,4286	6,5944	0,0507	395	445	3	4,8
0,125	1,0088	3,9411	3,7086	0,037	355	377	3,7	12,4
0,2	3,1246	16,0244	13,3599	0,0507	428	513	1.6	6,4

[a]Flux: mmol g^{-1} h^{-1}; [b]Exp.: experimental. One mole of lactose produces 4 moles of lactate, for the calculations the positive lactose flux is assumed. % Lactate flux = (lactate flux/lactose flux) *100. % biomass: D or μ / lactose flux *100.

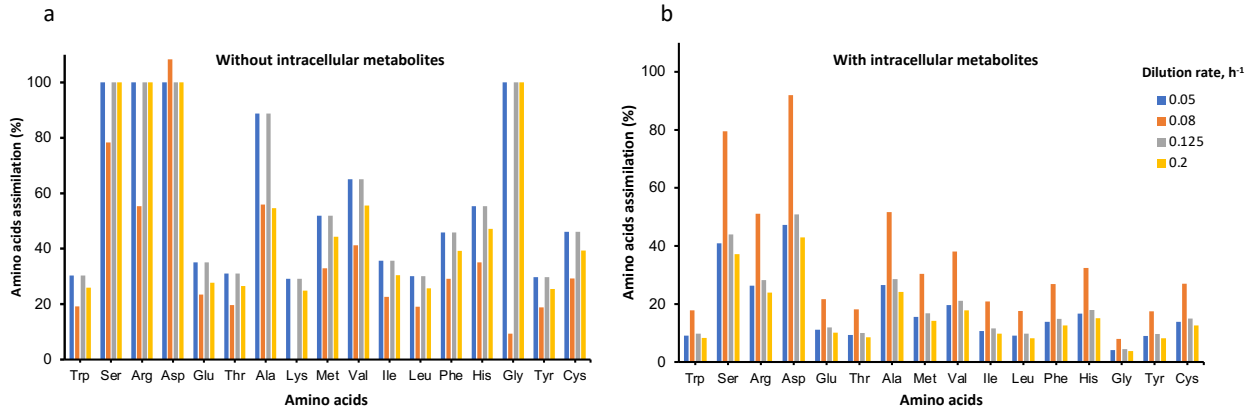

Figure 2. Simulated amino acid assimilation. The assimilation percentage of each amino acid at different dilution rates was evaluated a) with restrictions due to exchange reactions and b) with restrictions due to both exchange reactions and intracellular metabolite reaction determined with feasible solution. Trp: tryptophan, Ser: serine, Arg: arginine, Asp: aspartate, Glu: glutamate, Thr: Threonine, Ala: alanine, Lys: lysine, Met: methionine, Val: valine, ile: isoleucine, Leu: leucine, Phe: phenylalanine, His: histidine, Gly: glycine, Tyr: tyrosine, Cys: Cysteine.

DISCUSSION

In the present study, the culture conditions of the lactobacillus strain isolated from whey were established, to perform FBA associated with LA production, as the final product of bacterial metabolism. This strain was identified as *L. paracasei*, which is highly efficient in producing LA from whey (Mejia-Gomez & Balcazar 2020), which is a highly polluting waste product of the dairy industry (Zotta et al. 2020). The growth conditions in the continuous system of this bacterial strain only require 4 g L^{-1} of YE, as a source of amino acids. This condition favours the economic and technical feasibility of the bioprocess because this nutrient, involved in the production of LA, is approximately 38% of total production cost (Tejayadi & Cheryan 1995).

The *in-silico* simulations allowed the selection of biomass synthesis as the objective function that, despite presenting 60% overestimation, had a physiological behaviour more in line with the other two target functions evaluated. The increase in the simulated SGR with respect to the experimental one might be caused by the amino acid coefficients, since,

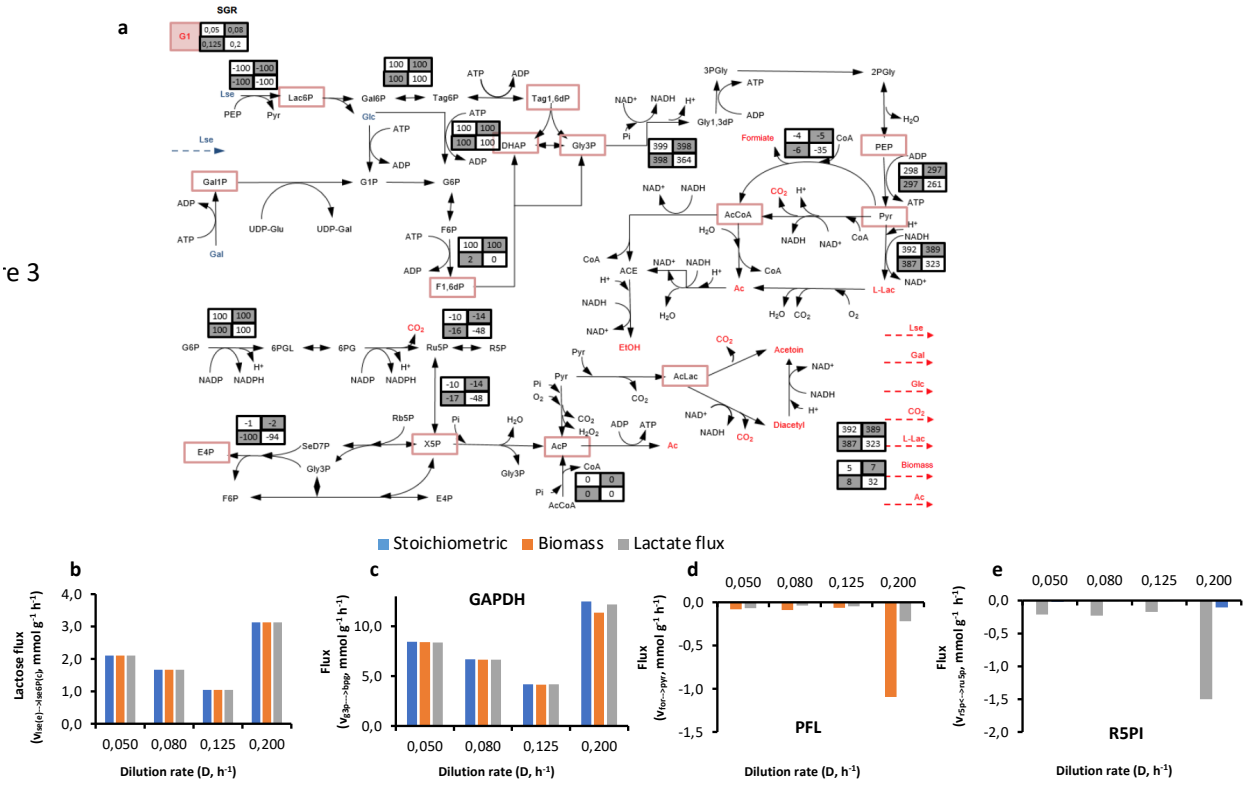

Figure 3. Metabolic map with restrictions caused by exchange reactions on the *i*Lca334_548 model. a) % flux i = (reaction flux i / lactose flux) × 100. Bar graph for lactose, b) GAPDH: Glyceraldehyde 3-phosphate dehydrogenase, c) PFL: pyruvate formate lyase, d) R5PI: Ribose-5-phosphate isomerase and e) fluxes using stoichiometric values and those obtained when evaluating biomass function and lactate flux. SGR: specific growth rate; PEP: phosphoenol pyruvate; SerAL: L-serine ammonia-lyase; AlaDH: alanine dehydrogenase; PK: pyruvate kinase; PC: pyruvate carboxylase; PDH: pyruvate dehydrogenase complex; PEPCK: phosphoenolpyruvate carbokinase; ADA: acetaldehyde dehydrogenase; ADH: alcohol dehydrogenase; PTA: phosphoacetyl transferase; AK: acetate kinase; PO: pyruvate oxidase; ALDC: acetolactato descarboxilasa; LDH: lactate dehydrogenase; MLE: malolactic enzyme: MDH: malate dehydrogenase; MAE1: mitochondrial malic enzyme; PPDK: pyruvate, phosphate dikinase; ALS: acetolactate synthase.

biomass synthesis in the different *Lactobacillus genus*, occurs from amino acids, lipids and other macromolecules, present in the culture medium (Novák & Loubiere 2000). Teusink et al. (2009) reported an increase in simulated SGR compared to the experimental increase of approximately 20%.

As in the present study, Teusink et al. (2009) reported that the best objective function for *L. plantarum* was biomass synthesis, one of the most widely applied objective functions because microorganisms tend to maximise biomass production (Lachance 2019, Feist & Palsson 2010). Biomass increases and lactate production decreases by increasing the dilution rate, possibly due to the increased availability of substrate that favours carbon flux towards biomass synthesis (Table I). The validation of the model shows that the *i*Lca334_548 model better predicts lactate flux than biomass synthesis (Table SV), which has been demonstrated for *L. lactis* (Novák & Loubiere 2000).

From the metabolic maps derived from the *i*Lca334_548 model under the condition of restrictions by exchange reactions (Fig. 3a) and the restrictions defined by intracellular

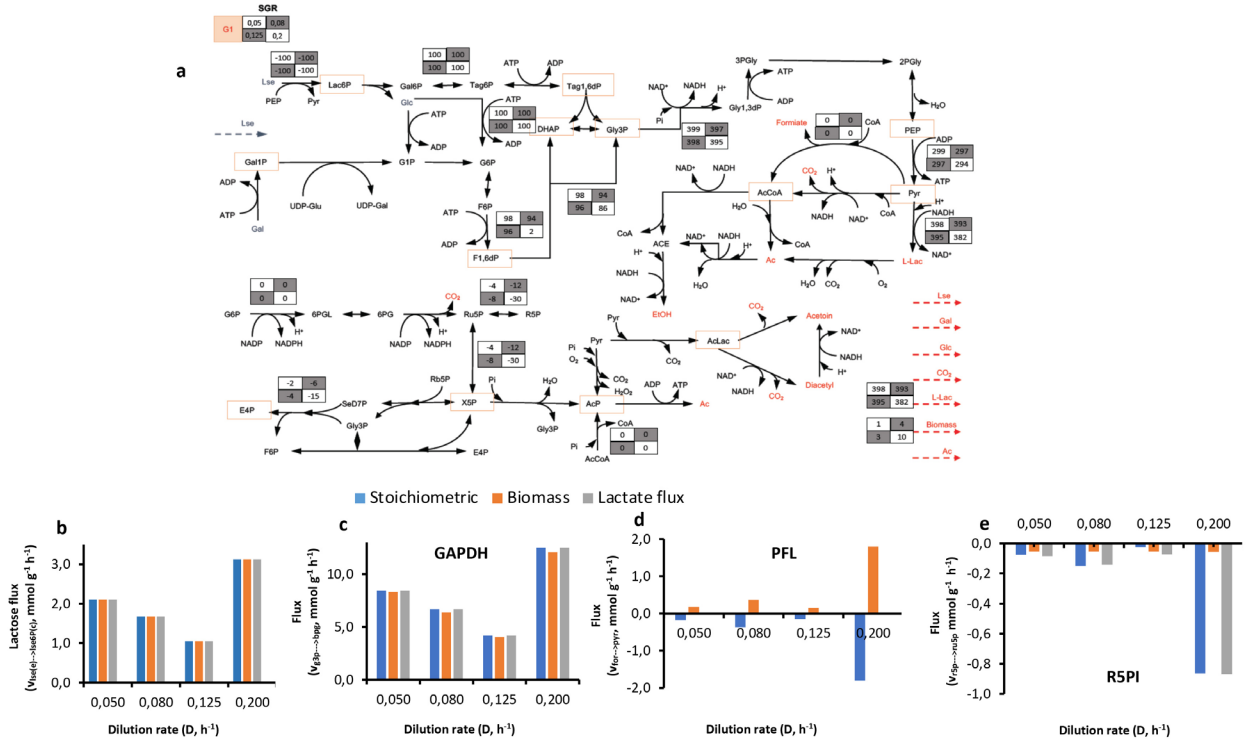

Figure 4. Metabolic map with restrictions caused by exchange reactions and intracellular metabolite concentration on the *i*Lca334_548 model. a) % flux i = (reaction flux i / lactose flux) × 100. Bar graph for lactose, b) GAPDH: Glyceraldehyde 3-phosphate dehydrogenase, c) PFL: pyruvate formate lyase, d) R5PI: Ribose-5-phosphate isomerase and e) fluxes using stoichiometric values and those obtained when evaluating biomass function and lactate flux. SGR: specific growth rate; PEP: phosphoenol pyruvate; SerAL: L-serine ammonia-lyase; AlaDH: alanine dehydrogenase; PK: pyruvate kinase; PC: pyruvate carboxylase; PDH: pyruvate dehydrogenase complex; PEPCK: phosphoenolpyruvate carbokinase; ADA: acetaldehyde dehydrogenase; ADH: alcohol dehydrogenase; PTA: phosphoacetyl transferase; AK: acetate kinase; PO: pyruvate oxidase; ALDC: acetolactato descarboxilasa; LDH: lactate dehydrogenase; MLE: malolactic enzyme: MDH: malate dehydrogenase; MAE1: mitochondrial malic enzyme; PPDK: pyruvate, phosphate dikinase; ALS: acetolactate synthase.

metabolites (Fig. 4a), it was determined that carbon flow is directed almost entirely to the catabolic processes, as validated in *Lactococcus lactis* (Novák & Loubiere 2000).

The dilution rate with high productivity (0.125 h^{-1}) was not limited to any of the metabolic fluxes but to the operational conditions of the continuous culture system (Fig. 3). Similar fluxes were obtained for dilution rates of 0.05, 0.08 and 0.125 h^{-1}, which approximate the experimental and/or stoichiometric values (Fig. 3b). There were lower fluxes at a higher dilution rate, which is characteristic of continuous systems, and provided greater carbon availability in the medium, leading to a homofermentative metabolism; this was consistent with the decrease in the activity of glyceraldehyde-3 phosphate dehydrogenase (GAPDH) (Fig. 3c). This enzyme increases the concentration of phosphate trioses, which are strong PFL inhibitors, thus guaranteeing a homofermentative metabolism. During the evaluation of flux distribution, flux through GAPDH does not respond to this hypothetical decrease in activity. In contrast, a higher GAPDH flux did not substantially changed flux through PFL (Fig. 3d). This would indicate that the glycolytic flux is not under the control of GAPDH because this metabolism remains homofermentative when there should be a mixed acid metabolism to achieve more ATP per

mole of carbohydrate when low dilution rates are involved.

The flux of R5PI at a dilution rate of 0.2 h^{-1} is directed to the formation of ribose-5-phosphate in comparison with the other dilution rates, particularly when the objective biomass function is maximised (Fig. 3e). This may partially explain the high biomass formation at this dilution rate as this metabolite is a precursor for nucleotide synthesis.

Some authors have reported that, in a continuous system, mixed acid metabolism is observed as dilution rate decreases, which consists of the production of lactic, formic and acetic acid or ethanol due to the action of the enzyme PFL (Melchiorsen et al. 2001) in *Lactococcus lactis* (Flahaut et al. 2013). This behaviour was not observed in the *i*Lca334_548 model results, initially taking only the restrictions that could be attributable to the exchange reactions with the culture medium (Fig. 3), and subsequently, when the intracellular metabolites considered in the restriction system were considered (Fig. 4). Greater biomass synthesis and lower LDH flux are observed in the metabolic map of Fig. 3a with respect to the metabolic map presented in Fig. 4a. The latter could be explained by the flux through PFL presented in Fig. 3a and absent in Fig. 4a. No ethanol or acetate was detected at the experimental level to consider a mixed metabolism. The increase in biomass observed in Figure 3a can be attributed to the formation of more acetyl CoA in the reaction catalysed by PFL, which is a precursor of fatty acid, lysine and peptidoglycan synthesis (Nordkvist et al. 2003, Teusink et al. 2006).

In the metabolic map, that included the restrictions of intracellular metabolite concentrations (Fig. 4a), almost all fluxes were zero and maximum lactate conversion was achieved. Moreover, the flux of pyruvate kinase (PK) did not change for the two conditions that were evaluated (Fig. 3 and Fig. 4); therefore, pyruvate provided by glycolysis was constant. Pyruvate present in the LDH reaction is the sum of the pyruvate from the PK and PTS^{LAC} system.

In the robustness analysis, the model showed a good fit to the experimental data where C:N ratio was evaluated. At a 5:1 ratio and a dilution rate of 0.125 h^{-1}, the lactate percentage flows were similar and close to the theoretical ones (400), both, for the model that considered intracellular metabolite flows, and for the one where it was not present (395 and 387 respectively, Fig. 3a and Fig. 4a).

The increase in restrictions due to the fluxes in intracellular metabolites requires the model to have a smaller solution space. This may be interpreted as a lower rate of amino acid metabolism that translates to a lower rate of biomass formation and higher lactate production. These data agree with the flows modelled in Fig. 3a and Fig. 4a. They also coincide with the experimental findings of the continuous system shown in Table I, where higher biomass lowers AL production. Further, Teusink et al. (2006) affirmed that when the models are more restricted, they become more descriptive and less predictive. Nevertheless, restricting the flows and optimising the biomass yield maximises efficiency, which is the main driving force of evolution.

The amino acids serine, aspartate and arginine, are in a high concentration in the yeast extract (Table SIII) and present assimilation of over 60% in the model without intracellular metabolites and 40% in the model with metabolite intracellular. Regardless of the dilution rate, the amino acid contribution to pyruvate formation is evident because in the model with intracellular restrictions, there is higher lactate production at the expense of biomass formation (Fig 4a). In the model

without intracellular restrictions, there is higher biomass, possibly because these amino acids (asp, ala, arg) could be leaded to the production of ATP, and therefore there is a lower production of lactate (Fig. 3a) (Fernández & Zuñiga 2006, Zhang et al. 2012).

In *in-silico* simulations, the high assimilation of some amino acids (Figure 2) may be associated with the formation of pyruvate through transamination reactions of alanine and aspartate mainly (Liu 2003), as well as the accumulation of pyruvate due to deamination of serine (Liu et al. 2003). The carbon skeleton of these amino acids is used for the production of lactate and flavor compounds through the central metabolism of carbohydrates, without the concomitant formation of ATP (Teusink et al. 2006). In the *i*Lca334_548 model, the consumption of serine (reaction 1), aspartate (reactions 2 and 3) and alanine (4) give pyruvate and then convert to lactate: ser_L[c] -> NH3[c] + pyr[c] (1); akg[c] + asp_L[c] <=> glu_L[c] + oaa[c] (2); oaa[c] + h+[c] -> co2[c] + pyr[c] (3); NADH[c] + NH3[c] + pyr[c] + H+[c] <=> h2o[c] + NAD[c] + ala_L[c] (4). Arginine is converted to aspartate by reactions 5 and 6 and finally transformed to pyruvate by reactions 2 and 3. argsuc[c] <=> arg_L[c] + fum[c] (5); ATP[c] + asp_L[c] + citr_L[c] <=> PPi[c] + AMP[c] + argsuc[c] (6)

No significant changes in amino acid metabolism were observed at the 0.08 h^{-1} dilution rate (Fig. 2). If the lactose flow is zeroed in the model, the specific growth rate is determined by the amino acid flow present at the defined dilution rate. The same specific growth rate (0.052 h^{-1}) was obtained with and without restrictions due to intracellular metabolites. This latter implies that a similar amino acid metabolism gives rise to the same rate of biomass generation. When the dilution rate is higher than 0.052 h^{-1}, the carbohydrate source is diverted to biomass formation (Oliveira et al. 2005).

The higher rate of biomass formation (Fig. 3a) is attributed to a higher rate of amino acid metabolism (Fig. 2a) as well as the flow that pyruvate formate lyase takes to form acetyl-CoA, an essential intermediate in the metabolism of lipids and the formation of biomass. The latter leads to a reduction in the concentration of pyruvate and therefore, the concentration of lactate.

CONCLUSIONS

The *i*Lca334_548 model showed a physiological behaviour appropriate to the experimental data for *L. paracasei* and lactate production was associated with the catabolism of amino acids. It is clear that at the level of a complex medium such as whey supplemented with YE, the flows that should be enhanced, according to the metabolism of the microorganism, are those associated with the catabolism of amino acids that give rise to more pyruvate because glycolysis yields have already reached the maximum expected level. Increasing the restrictions due to intracellular metabolites somewhat optimises the use of amino acids in biomass synthesis and allows the amino acid pool to be directed toward lactate production.

Acknowledgments

This work was supported by sustainability grants of Biotransformation and GENMOL Groups from Universidad de Antioquia.

REFERENCES

ALTIOK D, TOKATLI F & HARSA S. 2006. Kinetic modelling of lactic acid production from whey by *Lactobacillus casei* (NRRL B-441). Chem Technol Biotechnol 81(7): 1190-1197.

ALVAREZ MM, AGUIRRE-EZKAURIATZA EJ, RAMÍREZ-MEDRANO A & RODRÍGUEZ-SÁNCHEZ A. 2010. Kinetic analysis and

mathematical modelling of growth and lactic acid production of *Lactobacillus casei* var. rhamnosus in milk whey. J Dairy Sci 93(12): 5552-5560.

ALVES EP, MORIOKA L & SUGUIMOTO HH. 2019. Comparison of bioethanol and beta-galactosidase production by Kluyveromyces and Saccharomyces strains grown in cheese whey. In J Dairy Technol 72(3): 409-415.

AHMAD T ET AL. 2019. Treatment and utilization of dairy industrial waste: A review. Trends Food Sci Technol 88: 361-372.

CASTRO-AGUIRRE E, IÑIGUEZ-FRANCO F, SAMSUDIN H, FANG X & AURAS R. 2016. Poly (lactic acid) - Mass production, processing, industrial applications, and end of life. Adv Drug Deliv Rev 107: 333-366.

DUROT M, BOURGUIGNON PY & SCHACHTER V. 2009. Genome-scale models of bacterial metabolism: reconstruction and applications. FEMS Microbiol Rev 33(1): 164-190.

EDWARDS JS, IBARRA RU & PALSSON BO. 2001. In silico predictions of Escherichia coli metabolic capabilities are consistent with experimental data. Nat Biotechnol 19(2): 125-130.

EDWARDS JS & PALSSON BO. 2000. Robustness Analysis of the Escherichiacoli Metabolic Network. Biotechnol Prog 16(6): 927-939.

FEIST AM, HERRGÅRD MJ, THIELE I, REED JL & PALSSON BØ. 2009. Reconstruction of biochemical networks in microorganisms. Nat Rev Microbiol 7(2): 129-143.

FEIST AM & PALSSON BO. 2010. The biomass objective function. Curr Opin Microbiol 13(3): 344-349.

FERNÁNDEZ M & ZÚÑIGA M. 2006. Amino acid catabolic pathways of lactic acid bacteria. Crit Rev Microbiol 32(3): 155-183.

FLAHAUT NA, WIERSMA A, VAN DE BUNT B, MARTENS DE, SCHAAP PJ, SIJTSMA L, DOS SANTOS VA & DE VOS WM. 2013. Genome-scale metabolic model for *Lactococcus lactis* MG1363 and its application to the analysis of flavor formation. Appl Microbiol Biotechnol 97(19): 8729-8739.

FU W & MATHEWS AP. 1999. Lactic acid production from lactose by *Lactobacillus plantarum*: kinetic model and effects of pH, substrate, and oxygen. Biochem Eng J 3(3): 163-170.

GÄNZLE MG, VERMEULEN N & VOGEL RF. 2007. Carbohydrate, peptide and lipid metabolism of lactic acid bacteria in sourdough. Food Microbiol 24(2): 128-138.

GÄNZLE MG. 2015. Lactic metabolism revisited: metabolism of lactic acid bacteria in food fermentations and food spoilage. Curr Opin Food Sci 2: 106-117.

GE XY, XU Y, CHEN X & ZHANG LY. 2015. Regulation of metabolic flux in *Lactobacillus casei* for lactic acid production by overexpressed ldhL gene with two-stage oxygen supply strategy. J Microbiol Biotechnol 25(1): 81-88.

GONZÁLEZ-VARA A, PINELLI D, ROSSI M, FAJNER D, MAGELLI F & MATTEUZZI D. 1996. Production of l(+) and d(-) lactic acid isomers by *Lactobacillus casei* subsp. casei DSM 20011 and *Lactobacillus coryniformis* subsp. torquens DSM 20004 in continuous fermentation. J Ferment Bioeng 81(6): 548-552.

LACHANCE JC, LLOYD CJ, MONK JM, YANG L, SASTRY AV, SEIF Y, PALSSON BO, RODRIGUE S, FEIST AM, KING ZA & JACQUES PÉ. 2019. BOFdat: Generating biomass objective functions for genome- scale metabolic models from experimental data. PLoS Comput Biol 15(4): 1-20.

LIU SQ. 2003. Practical implications of lactate and pyruvate metabolism by lactic acid bacteria in food and beverage fermentations. Int J Food Microbiol 83(2): 115-131.

LIU SQ, HOLLAND R, MCJARROW P & CROW VL. 2003. Serine metabolism in *Lactobacillus plantarum*. Int J Food Microbiol 89(2-3): 265-273.

LUO B, GROENKE K, TAKORS R, WANDREY C & OLDIGES M. 2007. Simultaneous determination of multiple intracellular metabolites in glycolysis, pentose phosphate pathway and tricarboxylic acid cycle by liquid chromatography - mass spectrometry. J Chromatogr A 1147(2): 153-164.

MACHADO D, ANDREJEV S, TRAMONTANO M & PATIL KR. 2018. Fast automated reconstruction of genome-scale metabolic models for microbial species and communities. Nucleic Acids Res 46(15): 7542-7553.

MEJIA-GOMEZ CE & BALCÁZAR N. 2020. Isolation, characterisation and continuous culture of *Lactobacillus* spp. and its potential use for lactic acid production from whey. Food Sci Technol 40(4): 1021-1028.

MELCHIORSEN CR, JENSEN NB, CHRISTENSEN B, VAEVER JOKUMSEN K & VILLADSEN J. 2001. Dynamics of pyruvate metabolism in *Lactococcus lactis*. Biotechnol Bioeng 74(4): 271-279.

NAVID A. 2021. Curating COBRA Models of Microbial Metabolism. Methods Mol Biol 2349: 321-338.

NORDKVIST M, JENSEN NB & VILLADSEN J. 2003. Glucose metabolism in *Lactococcus lactis* MG1363 under different aeration conditions: requirement of acetate to sustain growth under microaerobic conditions. Appl Environ Microbiol 69(6): 3462-3468.

NOVÁK L & LOUBIERE P. 2000. The metabolic network of *Lactococcus lactis*: Distribution of 14C-Labeled

substrates between catabolic and anabolic pathways. J Bacteriol 182(4): 1136-1143.

OLIVEIRA AP, NIELSEN J & FÖRSTER J. 2005. Modeling *Lactococcus lactis* using a genome-scale flux model. BMC Microbiol 5(1): 39.

PANIKOV NS. 2021. Genome-Scale Reconstruction of Microbial Dynamic Phenotype: Successes and Challenges. Microorganisms 9(11): 2352.

PARMJIT S, PANESAR P, JOHN F, KENNEDY JF, CHARLES J, KNILL CJ & KOSSEVA M. 2010. Production of L(+) lactic acid using *Lactobacillus casei* from whey. Braz Arch Biol Technol 53(1): 219-226.

PEREIRA B, MIGUEL J, VILAÇA P, SOARES S, ROCHA I & CARNEIRO S. 2018. Reconstruction of a genome-scale metabolic model for Actinobacillus succinogenes 130Z. BMC Syst Biol 12(61): 1-12.

PINU FR, VILLAS-BOAS SG & AGGIO R. 2017. Analysis of Intracellular Metabolites from Microorganisms: Quenching and Extraction Protocols. Metabolites 7(4): 1-20.

RESEARCH AND MARKETS. 2017. Global Lactic Acid Market Size, Market Share, Application Analysis, Regional Outlook, Growth Trends, Key Players, Competitive Strategies and Forecasts, 2015 to 2022. https://www.researchandmarkets.com/research/3n8b8s/global_lactic.

RICCIARDI A, IANNIELLO RG, PARENTE E & ZOTTA T. 2015. Modified chemically defined medium for enhanced respiratory growth of *Lactobacillus casei* and *Lactobacillus plantarum* groups. J Appl Microbiol 119(3): 776-785.

SCHELLENBERGER J ET AL. 2011. Quantitative prediction of cellular metabolism with constraint based models: the COBRA Toolbox v2.0. Nat Protoc 6: 1290-1307.

SMITH EA, MYBURGH J, OSTHOFF G & DE WIT M. 2014. Acceleration of yoghurt fermentation time by yeast extract and partial characterisation of the active components. J Dairy Res 81(4): 417-423.

TAVARIA FK, DAHL S, CARBALLO FJ & MALCATA FX. 2002. Amino acid catabolism and generation of volatiles by lactic acid bacteria. J Dairy Sci 85(10): 2462-2470.

TEJAYADI S & CHERYAN M. 1995. Lactic acid from cheese whey permeates. Productivity and economics of a continuous membrane bioreactor. Appl Microbiol Biotechnol 43(2): 242-248.

TEUSINK B, WIERSMA A, JACOBS L, NOTEBAART RA & SMID EJ. 2009. Understanding the Adaptive Growth Strategy of *Lactobacillus plantarum* by In Silico Optimisation. PLoS Comput Biol 5(6): e1000410.

TEUSINK B, WIERSMA A, MOLENAAR D, FRANCKE C, DE VOS WM, SIEZEN RJ & SMID EJ. 2006. Analysis of growth of *Lactobacillus plantarum* WCFS1 on a complex medium using a genome-scale metabolic model. J Biol Chem 281(52): 40041-40048.

VINAY-LARA E, HAMILTON JJ, STAHL B, BROADBENT JR, REED JL & STEELE JL. 2014. Genome-scale reconstruction of metabolic networks of *Lactobacillus casei* ATCC 334 and 12A. PLoS ONE 9(11): e110785.

WATTHANASAKPHUBAN N, VIRGINIA LJ, HALTRICH D & PETERBAUER C. 2021. Analysis and reconstitution of the menaquinone biosynthesis pathway in Lactiplantibacillus plantarum and Lentilactibacillus buchneri. Microorganisms 9(7): 1476.

WEGKAMP A, TEUSINK B, DE VOS WM & SMID EJ. 2010. Development of a minimal growth medium for *Lactobacillus plantarum*. Lett Appl Microbiol 50(1): 57-64.

XAVIER JC, PATIL KR & ROCHA I. 2017. Integration of Biomass Formulations of Genome-Scale Metabolic Models with Experimental Data Reveals Universally Essential Cofactors in Prokaryotes. Metab Eng 39: 200-208.

YASMIN A, BUTT MS, SAMEEN A & SHAHID M. 2013. Physicochemical and amino acid profiling of cheese whey. Pak J Nutr 12(5): 455-459.

YOUSOFSHAHI M, ULLAH E, STERN R & HASSOUN S. 2013. MC3: a steady-state model and constraint consistency checker for biochemical networks. BMC Syst Biol 7: 129.

ZHANG J, WU C, DU G & CHEN J. 2012. Enhanced acid tolerance in *Lactobacillus casei* by adaptive evolution and compared stress response during acid stress. Biotechnol Bioprocess Eng 17(2): 283-289.

ZOTTA T, PARENTE E & RICCIARDI A. 2017. Aerobic metabolism in the genus *Lactobacillus*: impact on stress response and potential applications in the food industry. J Appl Micro 122(4): 857-869.

ZOTTA T, SOLIERI L, IACUMIN L, PICOZZI C & GULLO M. 2020. Valorization of cheese whey using microbial fermentations. Appl Microbiol Biotechnol 104: 2749-2764.

SUPPLEMENTARY MATERIAL

Appendix S1
Figure S1
Tables SI, SII, SIII, SIV, SV
Appendix S2

How to cite
MEJÍA-GOMEZ CE, RIOS-ESTEPA R, GONZALEZ-LOPEZ LA & BALCAZAR-MORALES N. 2022. An experimental and *in silico* analysis of *Lacticaseibacillus paracasei* isolated from whey shows an association between lactate production and amino acid catabolism. An Acad Bras Cienc 94: e20211071. DOI 10.1590/0001-3765202220211071.

Manuscript received on July 29, 2021;
accepted for publication on December 7, 2021

CARLOS EDUARDO MEJÍA-GOMEZ[1]
https://orcid.org/0000-0002-1413-9447

RIGOBERTO RIOS-ESTEPA[2]
https://orcid.org/0000-0002-3287-7056

LUIS ALBERTO GONZALEZ-LOPEZ[3]
https://orcid.org/0000-0002-4935-3320

NORMAN BALCAZAR-MORALES[4]
https://orcid.org/0000-0002-1860-1176

[1]Grupo de Biotransformación, Escuela de Microbiología, Universidad de Antioquia, Calle 70, N° 52-21, 050010 Medellin, Colombia

[2]Grupo de Bioprocesos, Facultad de Ingeniería, Universidad de Calle 70, N° 52-21, 050010 Medellin, Colombia

[3]Grupo de Química Orgánica de Productos Naturales, Facultad de Ciencias Exactas y Naturales, Universidad de Antioquia, Calle 70, N° 52-21, 050010 Medellin, Colombia

[4]Grupo de Genética Molecular y Departamento de Fisiología y Bioquímica, Facultad de Medicina, Universidad de Antioquia, Calle 62 N° 52-59, 050010 Medellín, Colombia

Correspondence to: **Norman Balcazar-Morales**
E-mail: norman.balcazar@udea.edu.co

Author contributions

Carlos Eduardo Mejia-Gomez: Conceptualization, Methodology, formal analysis, writing - reviewing & editing, Luis Alberto Gonzales-Lopez: Methodology, Rigoberto Rios-Estepa: formal analysis, writing - reviewing & editing, Norman Balcazar-Morales: Conceptualization, formal analysis, writing - review, editing & supervision.